RSC Advances

PAPER

View Article Online
View Journal | View Issue

Cite this: *RSC Adv.*, 2020, **10**, 14218

Simultaneous electrochemical detection of levodapa, paracetamol and L-tyrosine based on multi-walled carbon nanotubes

Zai-Yu Li,[a] Dan-Yang Gao,[a] Zhi-Yong Wu *[b] and Shuang Zhao *[a]

Received 10th January 2020
Accepted 31st March 2020

DOI: 10.1039/d0ra00290a

rsc.li/rsc-advances

Herein multi-walled carbon nanotubes (MWCNTs) were processed by ultrasonication and freeze-drying method. The morphology of the processed MWCNTs was examined by scanning electron microscopy. An original electrochemical sensor for the simultaneous detection of levodapa (LD), paracetamol (PA) and L-tyrosine (Tyr) was developed by dropcasting a mixture of processed MWCNTs and Nafion on a glassy carbon electrode. The as-prepared sensor was studied by cyclic voltammetry and differential pulse voltammetry. The peak currents of LD, PA and Tyr significantly increased compared to those obtained at bare glassy carbon electrodes or unprocessed MWCNTs modified electrodes. The peaks of LD, PA and Tyr were well-defined and obviously separated from each other. The linear ranges for detection of LD, PA and Tyr were 2.0–300.0, 2.0–180.0, and 2.0–120.0 μM, with a detection limit of 0.6, 0.5 and 0.8 μM (S/N = 3), respectively. Finally, the sensor was applied to detect LD, PA and Tyr in serum samples, and the results were satisfactory.

Introduction

Parkinson's disease (PD) is the second most common neurodegenerative disease, and causes the progressive deterioration of the motor system. Levodopa (LD) is the most potent medicine in PD treatment.[1,2] Along with its effectiveness, LD might cause a series of side effects.[3] Hence, the detection of LD is essential for controlling its dose. Several methods for the detection of LD in medicines or biological samples have been reported, including chromatography,[4] spectroscopy[5] and electrical analysis.[6–10]

Pain is a common problem in PD patients. Non-steroidal anti-inflammatory drugs, such as paracetamol (PA) and aspirin, are commonly used to relieve PD-related pain.[11–13] When administered in a suitable dose, PA has excellent safety. Excessive PA may cause the accumulation of toxic metabolites, resulting in severe time-dependent hepatotoxicity and nephrotoxicity.[11] At present, various methods have been introduced for the detection of PA, such as capillary electrophoresis,[14] high-performance liquid chromatography (HPLC),[15] spectroscopy[16] and electrochemical techniques.[17,18]

L-tyrosine (Tyr) is an amino acid found in the diet that is involved in producing catecholamines such as dopamine and adrenaline. The synthesis of catecholamines is highly regulated in the body and tyrosine hydroxylase converts Tyr into LD. After administration of LD in PD, the levels of Tyr would reduce.[19] Orthostatic hypotension (OH) is a common and disabling symptom affecting PD patients.[20] Studies have demonstrated that supplementing Tyr may increase norepinephrine and minimize OH in PD.[21,22] Different kinds of methods have been developed for the detection of Tyr such as HPLC,[23] capillary electrophoresis[24] and others.[25–27]

All of LD, PA and Tyr are commonly used drugs in PD treatment. Especially, Tyr and LD have quite similar chemical structures and physiological functions. Both of them are essential for synthesizing dopamine and some other important biological compounds in human body. So it is very interesting and significant to establish a simple and sensitive method for simultaneous determination of LD, PA and Tyr. The electrochemical approach is a promising choice to realize this goal, due to its prompt response, high sensitivity and selectivity, simple operation, and low cost. Moreover, it is assumed that the redox reactions occurring in the biological systems and at the electrode surfaces have similar principles.[28] However, the literature survey shows that there is only one electrochemical sensing platform for simultaneous determination of LD, PA and Tyr has been reported.[29] In that paper, a graphene and ethyl 2-(4-ferrocenyl-[1,2,3]triazol-1-yl)acetate modified carbon paste electrode was applied to detect LD in the presence of PA and Tyr using square wave voltammetry.

The carbon nanotubes (CNTs) have been extensively used to develop electrochemical sensors due to their high surface area, excellent electrical conductivity and catalytic properties,[30] since their discovery in 1991.[31] Herein, the multi-walled carbon

[a]*Chemistry Department, College of Sciences, Northeastern University, Wenhua Road 3-11, Shenyang, 110819 Liaoning, China. E-mail: zhaoshuang@mail.neu.edu.cn*
[b]*Research Center for Analytical Sciences, Chemistry Department, College of Sciences, Northeastern University, Wenhua Road 3-11, Shenyang, 110819 Liaoning, China. E-mail: zywu@mail.neu.edu.cn*

nanotubes (MWCNTs) were processed using ultrasonication and freeze-drying method. The processed MWCNTs interconnected and formed a 3D porous framework, which is propitious for electrochemical determination with rapid electron transfer and mass transfer. Then we fabricated a novel electrochemical sensor for simultaneous determination of LD, PA and Tyr based on the processed MWCNTs. In the end, we evaluated the analytical performance of the proposed sensors.

Experimental

Materials and apparatus

All chemicals used in this study were of analytical reagent grade. MWCNTs were purchased from Chengdu Organic Chemicals Co. Ltd., Chinese Academy of Sciences (China). Levodopa was purchased from Hefei Bomei Biological Technology Co., Ltd. (China). Paracetamol and L-Tyrosine were purchased from Aladdin reagent Co., Ltd. (Shanghai, China). Nafion (5 wt%) solution was obtained from Sigma-Aldrich. All solutions in the experiments were prepared in deionized water. Phosphate buffer solutions with different pH values (PBS, 0.1 M) were prepared by mixing stock standard solutions of 0.1 M NaH_2PO_4 and 0.1 M Na_2HPO_4.

All electrochemical experiments were conducted on a CHI 760E workstation (CH Instruments, Shanghai, China) with a three-electrode cell, which composed of a working electrode (glassy carbon electrode (GCE), $\Phi = 3$ mm), an Ag/AgCl reference electrode and a platinum wire counter electrode. Error bars represent one standard deviation of the means ($n = 3$). The morphology of the processed MWCNTs was characterized *via* scanning electron microscopy (SEM, Hitachi S3400N, Japan).

Pretreatment of MWCNTs

To obtain carboxyl functionalized MWCNTs and remove the impurities, the MWCNTs were oxidized in the mixture of concentrated H_2SO_4/HNO_3 (3 : 1 v/v, 98% and 70%, respectively). The mixture was subjected to ultrasonic treatment at 40 °C for 4 h, followed by centrifugation and extensive rinsing with distilled water until the pH of filtrate was neutral. The obtained products were dried at 60 °C for 12 h under vacuum.[32]

Processing of MWCNTs used for sensor fabrication

Prior to sensor fabrication, the carboxyl functionalized MWCNTs were processed by ultrasonication and freeze-drying methods.[33] 18 mg of carboxylated multi-walled carbon nanotubes were placed in 18 mL of deionized water, sonicated at 40 °C for 2 h, stirred at room temperature for 3 h, frozen overnight, and freeze-dried for 48 h for collection.

Fabrication of sensor

The GCE was first polished with 1.0 and 0.3 μm alumina powders on the polishing cloth. After each polishing step, it was ultrasonically cleaned with deionized water for 3 min. The processed GCE was dried with nitrogen for the following usage. 1.0 mg MWCNTs processed by ultrasonication and freeze-drying was dispersed in 1 mL 1% Nafion solution and sonicated to obtain a stable MWCNTs-Nafion suspension. Then 8 μL of MWCNTs-Nafion suspension was dropcasted on the surface of a cleaned GCE and dried in the air to obtain MWCNTs-Nafion/GCE. The carboxyl functionalized MWCNTs, which weren't processed by ultrasonication and freeze-drying, were also used to modify GCE using the same procedure for control experiments (marked as MWCNTs (unprocessed)-Nafion/GCE). All electrodes were stored in fridge at 4 °C when not in use.

Results and discussion

SEM of the processed MWCNTs

The morphology of MWCNTs after the ultrasonication and freeze-drying treatment was characterized by SEM. The porous and interconnected integrated framework of multi-walled carbon nanotubes can be clearly seen from Fig. 1, which exhibits a higher specific surface area and contributes to strong adsorption and rapid diffusion of analyte. Most of the carbon nanotubes are in fluffy and homogeneous single state, indicating that the dispersion of MWCNTs is improved after the ultrasonication and freeze-drying processing.

Electrochemical response of LD, PA and Tyr

The electrochemical responses of LD, PA and Tyr were characterized by cyclic voltammetry (CV) at different electrodes. Fig. 2 shows the CVs of 0.05 mM LD, 0.03 mM PA and 0.10 mM Tyr at (a) GCE, (b) MWCNTs (unprocessed)-Nafion/GCE and (c) MWCNTs-Nafion/GCE. Three tiny oxidation peaks of LD, PA and Tyr were observed at GCE (curve a). The resolution and intensity of these oxidation peaks were too low to realize the simultaneous detection of LD, PA and Tyr. At MWCNTs (unprocessed)-Nafion/GCE (curve b), the oxidation peaks of LD, PA and Tyr increased obviously. And the electrochemical reversibility of PA was improved, since the corresponding reduction peak of PA appeared. This indicated that MWCNTs were benefit to the electrochemical reactions of LD, PA and Tyr. At MWCNTs-Nafion/GCE (curve c), all the redox peaks of LD, PA and Tyr were significantly larger than those at MWCNTs (unprocessed)-Nafion/GCE. And the reduction peak potential of PA shifted positively.

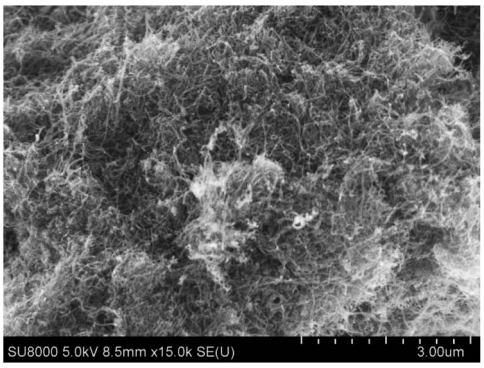

Fig. 1 SEM image of MWCNTs after the ultrasonication and freeze-drying treatment.

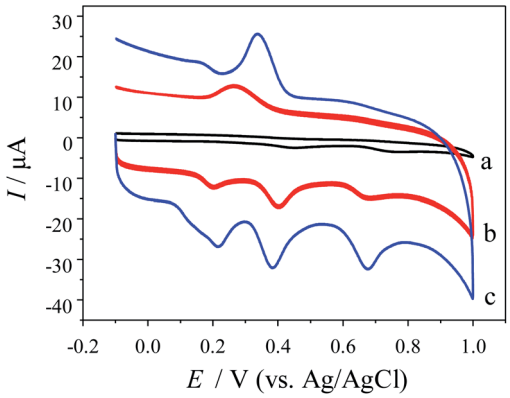

Fig. 2 Cyclic voltammograms of 0.05 mM LD, 0.03 mM PA and 0.10 mM Tyr in 0.1 M PBS (pH 7.0) at different electrodes: (a) GCE, (b) MWCNTs (unprocessed)-Nafion/GCE, (c) MWCNTs-Nafion/GCE. Scan rate: 100 mV s^{-1}.

This was because ultrasonication and freeze-drying made the MWCNTs fluffy and easily dispersed, thereby greatly enhancing their processability and circumventing the decline of excellent electrochemical properties induced by the aggregation. The well-defined oxidation peaks of LD, PA and Tyr were located at 212 mV, 393 mV and 683 mV, respectively. It was clearly indicated that MWCNTs-Nafion/GCE had an efficient catalysis towards the electrochemical reactions of LD, PA and Tyr. Both the separations of oxidation peaks and current responses at MWCNTs-Nafion/GCE were large enough for simultaneous determination of the above three analytes in mixture.

Optimization of MWCNTs-Nafion dosage

The influence of MWCNTs-Nafion film thickness on the oxidation peak currents of LD, PA and Tyr was examined. The thickness of MWCNTs-Nafion film was restricted by the volume of MWCNTs-Nafion suspension dropped on the GCE surface. Fig. 3 shows that all the oxidation peak currents of LD, PA and Tyr increased at first with suspension volume in the cause of the expansion of effective area of MWCNTs-Nafion/GCE, and then decreased indicating that a thicker MWCNTs-Nafion film results in a more difficult electrode response. The oxidation peak currents of LD, PA and Tyr peaked at 8 μL. Accordingly, the optimum volume of MWCNTs-Nafion suspension was 8 μL.

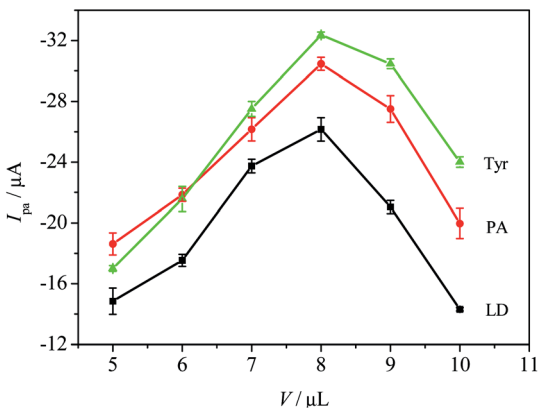

Fig. 3 The dependences of the oxidation currents of LD, PA and Tyr on the volume of MWCNTs-Nafion suspension in the presence of 0.05 mM LD, 0.03 mM PA and 0.10 mM Tyr in 0.1 M PBS (pH 7.0).

Effect of pH

The influence of pH on the redox reactions of LD, PA and Tyr was studied by CV in 0.1 M PBS with different pH value, at a scan rate of 100 mV s^{-1}. Fig. 4B reveals the variations of the oxidation currents with respect to pH. It is clearly shown that the oxidation currents of PA and Tyr peaked at pH 7.0, while the oxidation peak current of LD reduced gradually with pH from 5.0 to 9.0. Therefore, 0.1 M PBS (pH 7.0) was used in follow-up experiments. As

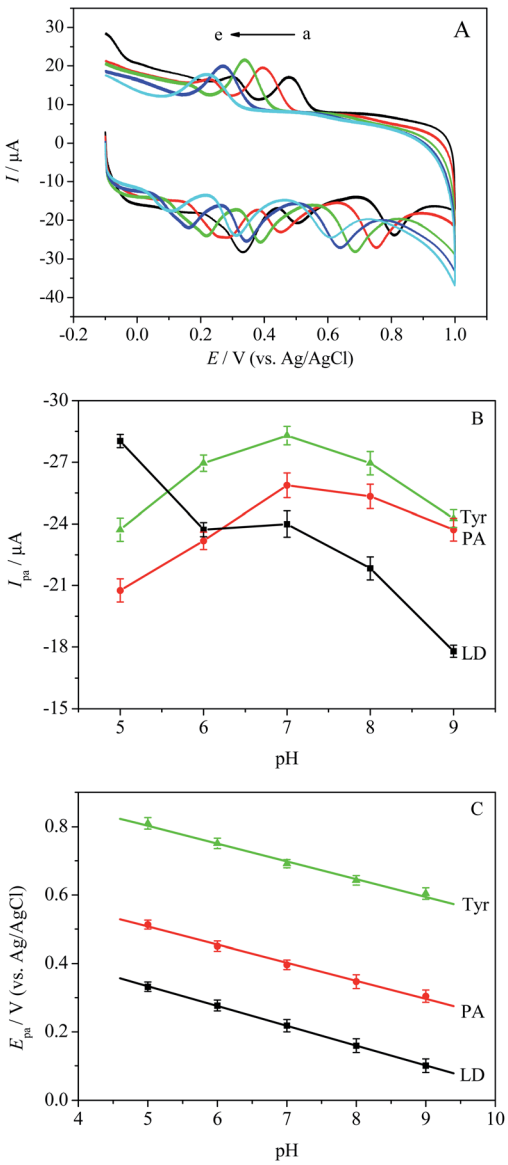

Fig. 4 (A) Cyclic voltammograms of MWCNTs-Nafion/GCE in 0.1 M PBS containing 0.05 mM LD, 0.03 mM PA and 0.10 mM Tyr at different pHs: from a to e was 5.0, 6.0, 7.0, 8.0 and 9.0. Scan rate: 100 mV s^{-1}. (B) Variations of the oxidation peak currents *vs.* pH. (C) Plot of oxidation peak potentials *vs.* pH.

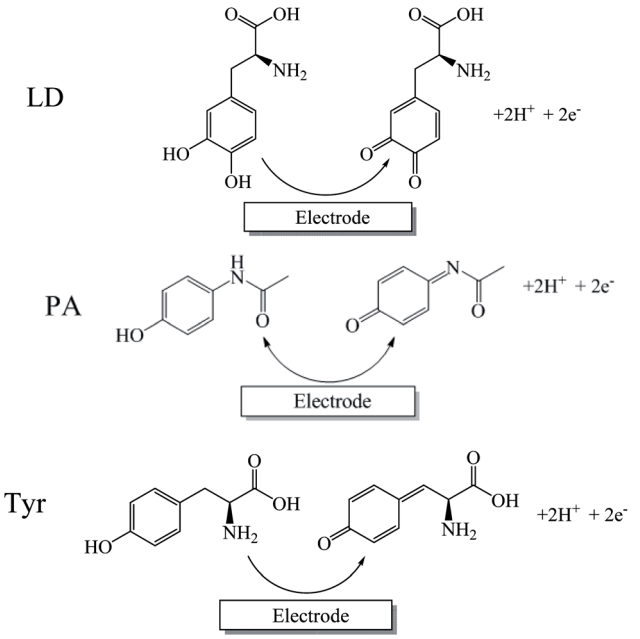

Scheme 1 The proposed electrochemical reaction mechanisms of LD, PA and Tyr.

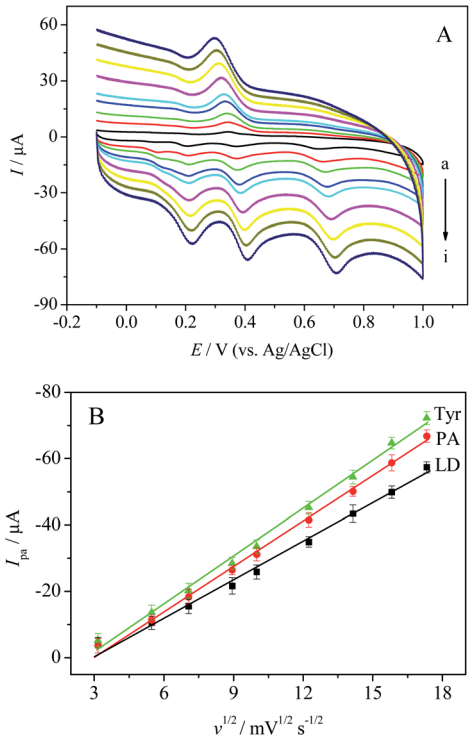

Fig. 5 (A) Cyclic voltammograms of MWCNTs-Nafion/GCE in 0.1 M PBS (pH 7.0) containing 0.05 mM LD, 0.03 mM PA and 0.10 mM Tyr at different scan rates (a–i: 10, 30, 50, 80, 100, 150, 200, 250, 300 mV s^{-1}). (B) Plots of oxidation peak currents *vs.* the square root of scan rates for LD, PA and Tyr.

shown in Fig. 4A, the increase of solution pH caused the negative shifts of the redox peak potentials of LD, PA and Tyr, which indicated the protons participating directly in the electrochemical reactions of LD, PA and Tyr. Fig. 4C shows the effect of pH on the oxidation peak potentials of LD, PA and Tyr. All the oxidation peak potentials of LD, PA and Tyr have the linear relationships with pH from 5.0 to 9.0 with the slopes of −58.0, −52.1 and −51.9 mV pH^{-1}, respectively. All the slopes approach the theoretical value given by the Nernst equation (−59.2 mV pH^{-1}) for equal number of electrons and protons involved reaction. With the reference of relevant literature,[34,35] the electrochemical reactions of LD, PA and Tyr can be expressed as Scheme 1.

Effect of scan rate

Furthermore, the influence of scan rate on the CVs of LD, PA and Tyr at MWCNTs-Nafion/GCE was explored in 0.1 M PBS. Fig. 5A shows the CVs in the mixture of 0.05 mM LD, 0.03 mM PA and 0.10 mM Tyr at different scan rates in the ranges of 10–300 mV s^{-1}. It is obviously observed that all the oxidation peak currents of LD, PA and Tyr increased linearly with the square root of scan rate. The linear regression equations of LD, PA and Tyr are I_{pa} (μA) = 3.818$\nu^{1/2}$ (mV s^{-1}) − 10.735 (R = 0.9968), I_{pa} (μA) = 3.777 $\nu^{1/2}$ (mV s^{-1}) − 10.849 (R = 0.9984) and I_{pa} (μA) = 4.816$\nu^{1/2}$ (mV s^{-1}) − 12.884 (R = 0.9975), respectively. The results indicated that all the electrochemical reactions of LD, PA and Tyr were diffusion control processes.

Individual detection of LD, PA and Tyr in ternary mixed solution

The individual detection of LD, PA or Tyr in their ternary mixed solution was investigated by differential pulse voltammetry (DPV) under optimized conditions. The DPV curves were recorded at MWCNTs-Nafion/GCE by changing one analyte's concentration, while those of other two analytes kept constant. Fig. 6A depicted that the oxidation peak currents of LD enhanced with its concentration in the range of 2.0 to 300.0 μM, while the oxidation peak currents of 0.01 mM PA and 0.01 mM Tyr kept nearly unchanged. The corresponding linear regression equation of LD was shown as I_{pa} (μA) = 0.0955c_{LD} (μM) − 0.327 (R = 0.9959), and the detection limit was estimated to be 0.6 μM at a signal-to-noise of 3. As shown in Fig. 6C, fixing the concentrations of LD and Tyr constant (0.01 mM), the oxidation peak currents of PA increased linearly with its concentration. The linear relationship for determination of PA is from 2.0 to 180.0 μM, and the linear regression equation was I_{pa} (μA) = 0.2723c_{PA} (μM) + 2.711 (R = 0.9976), with the detection limit of 0.5 μM. Similarly, Fig. 6E depicted the DPV responses of Tyr in the presence of 0.01 mM LD and 0.01 mM PA, which exhibited a linear relationship in concentration range of 2.0–120.0 μM, and its linear regression equation could be expressed as I_{pa} (μA) = 0.0344c_{Tyr} (μM) + 0.2456 (R = 0.9983), with the detection limit of 0.8 μM.

Table 1 showed the analytical performance comparison of MWCNTs-Nafion/GCE with some previous literatures for the determination of LD, PA and Tyr. As can be obtained from Table 1, the sensor fabricated in this work has better or comparable linear range and detection limit. Most important of all, MWCNTs-Nafion/GCE is a suitable sensor for the simultaneous determination of LD, PA and Tyr.

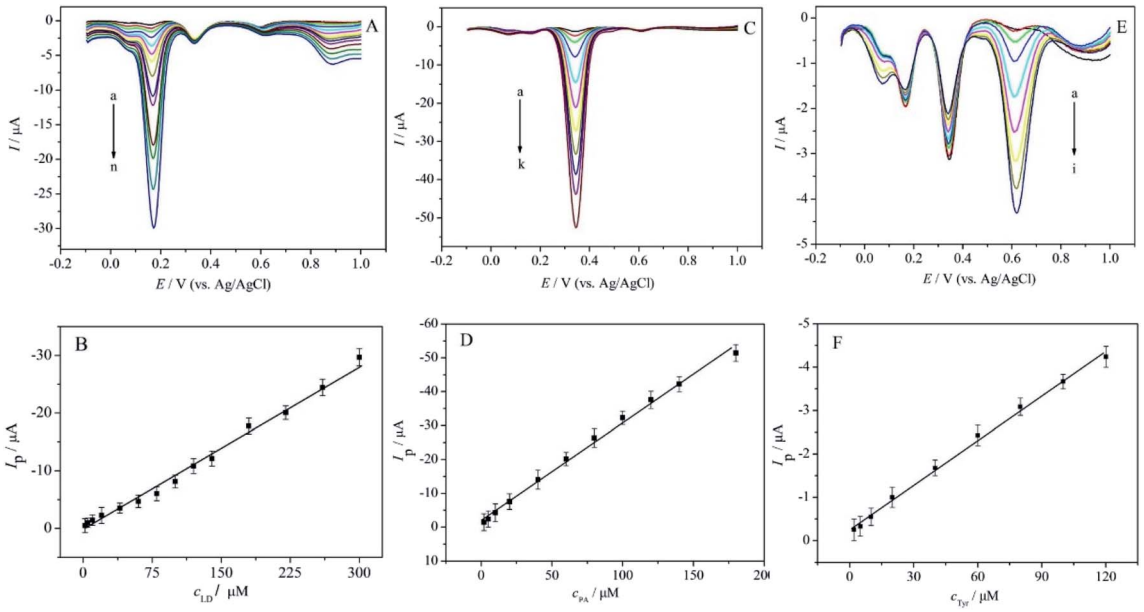

Fig. 6 Differential pulse voltammograms of MWCNTs-Nafion/GCE in 0.1 M PBS (pH 7.0) (A) in presence of 0.01 mM PA and 0.01 mM Tyr and different concentrations of LD (from a to n: 2.0–300.0 μM). (C) In presence of 0.01 mM LD and 0.01 mM Tyr and different concentrations of PA (from a to k: 2.0–180.0 μM). (E) In presence of 0.01 mM LD and 0.01 mM PA and different concentrations of Tyr (from a to k: 2.0–120.0 μM). (B, D and F) The calibration plots of the peak currents *vs.* concentrations of LD, PA and Tyr, respectively.

Simultaneous electrochemical determination of LD, PA and Tyr

The feasibility of MWCNTs-Nafion/GCE for the simultaneous determination of LD, PA and Tyr in ternary mixed solution was demonstrated by DPV. As can been seen in Fig. 7, when the concentration of LD, PA and Tyr increased simultaneously, their oxidation peak currents increased linearly with their concentrations. When the concentration was increased from 2.0 to 80.0 μM for LD, 2.0 to 18.0 μM for PA, and 2.0 to 140.0 μM for Tyr, the linear regression equations for LD, PA and Tyr are I_{pa} (μA) = 0.05394c_{LD} (μM)+ 0.4845 (R = 0.9990), I_{pa} (μA) = 0.4200c_{PA} (μM) − 0.1875 (R = 0.9995) and I_{pa} (μA) = 0.03643c_{Tyr} (μM) + 0.2788 (R = 0.9978), respectively. The results indicated that simultaneous determination of LD, PA and Tyr was feasible at MWCNTs-Nafion/GCE.

Reproducibility, stability and interference studies

The reproducibility and stability of MWCNTs-Nafion/GCE were investigated by measuring the current responses in 0.1 M PBS containing 0.05 mM LD, 0.03 mM PA and 0.10 mM Tyr. The relative standard deviations of 10 successive measurements using the same modified electrode were 3.5% for LD, 3.0% for PA and 3.8% for Tyr. This indicated that the reproducibility of MWCNTs-Nafion/GCE was excellent. Meanwhile, five different glassy carbon electrodes modified by the proposed method were independently applied for simultaneous determination of LD, PA and Tyr. The relative standard deviations were 4.0%, 3.7% and 4.3% for LD, PA and Tyr, respectively. The results also indicated that the electrode-to-electrode reproducibility of MWCNTs-Nafion/GCE was good. In addition, when MWCNTs-

Table 1 Comparisons of major characteristics at the various modified electrodes for the determination of LD, PA and Tyr

Modified electrode	Analyst	Linear range (μM)	Detection limit (μM)	Reference
Q/fMWCNT/MGCE	LD	0.9–85	0.38	34
fMWCNT/GCE	LD	0.7–100	0.25	35
AuNP-CMC-xGnP/GCE	LD	5–50	0.5	36
MWCNTs-Nafion/GCE	LD	2–300	0.6	This work
fMWCNT/GCE	PA	1–90	0.52	35
Lt/fMWCNT/MGCE	PA	0.9–80	0.78	37
CNTPE	PA	5–92.6	0.57	38
EFTA/CPE	PA	1–150	0.5	29
MWCNTs-Nafion/GCE	PA	2–80	0.5	This work
TiO_2-GR/GCE	Tyr	10–160	2.3	39
AuNPs/poly (trisamine)/GCE	Tyr	3.9–61.8	0.9	40
EFTA/CPE	Tyr	5–180	2	29
AuNPs/MWCNT/GCE	Tyr	0.4–80	0.21	41
MWCNTs-Nafion/GCE	Tyr	2–120	0.8	This work

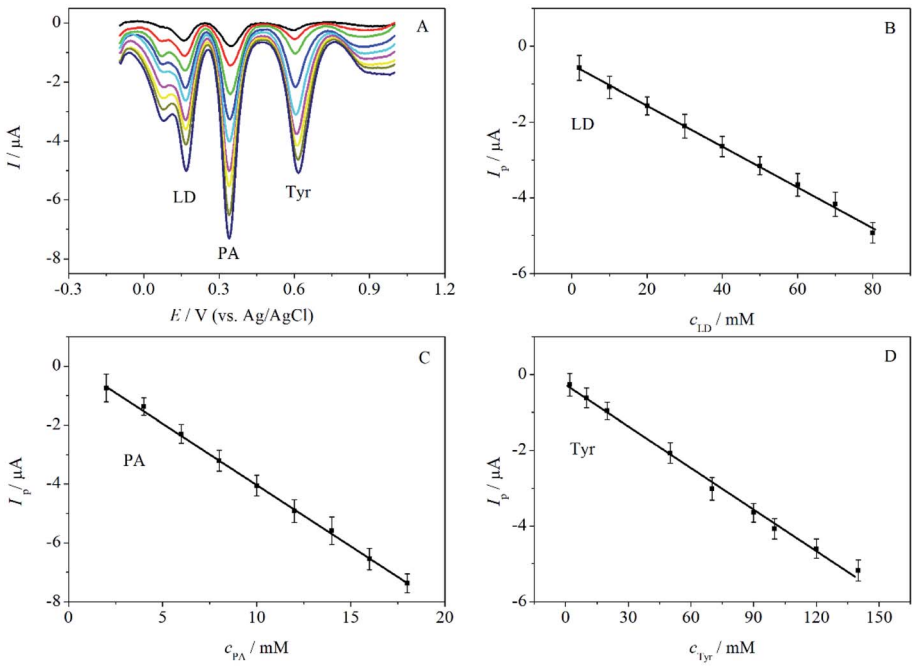

Fig. 7 (A) Differential pulse voltammograms of MWCNTs-Nafion/GCE in 0.1 M PBS (pH 7.0) containing different concentrations of LD (2.0–80.0 μM), PA (2.0–18.0 μM) and Tyr (2.0–140.0 μM). (B, C and D) The calibration plots of the peak currents *vs.* concentrations of LD, PA and Tyr, respectively.

Table 2 Determination of LD, PA and Tyr in human serum by MWCNTs-Nafion/GCE ($n = 5$)

	Added (μM)	Founded (μM)	Recovery (%)	RSD (%)
LD	10.0	10.2	102.0	3.5
	30.0	30.1	100.3	3.0
	50.0	49.1	98.2	2.6
PA	10.0	9.5	95.0	3.0
	30.0	29.5	98.3	2.7
	50.0	51.9	103.8	3.2
Tyr	10.0	9.6	96.0	3.8
	30.0	28.6	95.3	2.8
	50.0	52.3	104.6	3.2

Nafion/GCE was stored in a fridge at 4 °C for two weeks, it retained about 95.4%, 96.5% and 95.3% of the initial current of LD, PA and Tyr, respectively, indicating a relatively robust stability.

The ability to discriminate the analytes and interferents is a crucial indicator to evaluate the performance of sensor. In this work, the selectivity of MWCNTs-Nafion/GCE towards other species was investigated by DPV in 0.1 M PBS (pH 7.0) containing 0.01 mM LD, 0.005 mM PA and 0.03 mM Tyr. It was found that common inorganic ions such as 0.5 mM K^+, Na^+, Ca^{2+}, Zn^{2+}, Mg^{2+}, NO_3^-, Cl^-, SO_4^{2-} and CO_3^{2-} almost did not affect the responses of LD, PA and Tyr. The potential interferences existing in biological samples such as 0.3 mM glucose, lysine, histidine or arginine did not interfere significantly. Thus, the modified electrode has good selectivity for simultaneous determination of LD, PA and Tyr.

Real sample analysis

To prove the utility of MWCNTs-Nafion/GCE, the detection of LD, PA and Tyr were examined in human serum (diluted 50 times with 0.1 M pH 7.0 PBS) by the standard addition method. As shown in Table 2, the recoveries are 98.2% to 102.0%, 95.0% to 103.8%, and 95.3% to 104.6% for LD, PA and Tyr, respectively. These results demonstrate the feasibility of MWCNTs-Nafion/GCE in real sample analysis.

Conclusion

In summary, a novel electrochemical sensor was fabricated by drop casting multi-walled carbon nanotubes processed by ultrasonication and freeze-drying on the surface of glassy carbon electrode with Nafion as matrix. The modified electrode was used for simultaneous determination of LD, PA and Tyr. The preparation method is simple and low-cost. The fluffy and interconnected integrated structure of multi-walled carbon nanotubes provided an appropriate microenvironment for the electrochemical reaction of LD, PA and Tyr. The experimental results showed that the proposed modified electrode exhibited wide linear concentration range, high stability, good selectivity and reproducibility. The results of real sample analysis are satisfactory.

Conflicts of interest

There are no conflicts to declare.

Acknowledgements

This work was supported by the National Natural Science Foundation of China (No. 51909031), the Science and Technology Projects of Liaoning Province and the China Scholarship Council (201706085005).

Notes and references

1 J. Hardy and K. Gwinn-Hardy, *Science*, 1998, **282**, 1075.
2 R. Katzenschlager and W. Poewe, *Nat. Rev. Neurol.*, 2014, **10**, 128.
3 M. Sadikovic, B. Nigovic, S. Juric and A. Mornar, *J. Electroanal. Chem.*, 2014, **733**, 60.
4 J. D. Chi, Y. H. Ling, R. Jenkins and F. M. Li, *J. Chromatogr. B: Anal. Technol. Biomed. Life Sci.*, 2017, **1054**, 1.
5 M. F. Abdel-Ghany, L. A. Hussein, M. F. Ayad and M. M. Youssef, *Spectrochim. Acta, Part A*, 2017, **171**, 236.
6 S. Tajik, M. A. Taher and H. Beitollahi, *Electroanalysis*, 2014, **26**, 796.
7 Y. Shoja, A. A. Rafati and J. Ghodsi, *Mater. Sci. Eng. C*, 2016, **58**, 835.
8 H. Beitollahi and F. G. Nejad, *Electroanalysis*, 2016, **28**, 2237.
9 J. Ghodsi, A. A. Rafati and Y. S. Ghodsi, *Anal. Bioanal. Chem.*, 2016, **408**, 3899.
10 M. G. Hosseini, M. Faraji, M. M. Momeni and S. Ershad, *Microchim. Acta*, 2011, **172**, 103.
11 D. N. Bateman and A. Vale, *Medicine*, 2016, **44**, 190.
12 O. Skogar and J. Lokk, *J. Multidiscip. Healthc.*, 2016, **9**, 469.
13 C. J. Locke, S. A. Fox, G. A. Caldwell and K. A. Caldwell, *Neurosci. Lett.*, 2008, **439**, 129.
14 T. Hložek, T. Křížek, P. Tůma, M. Bursová, P. Coufal and R. Čabala, *J. Pharm. Biomed. Anal.*, 2017, **145**, 616.
15 V. Ohriac, D. Cimpoesu, A. F. Spac, P. Nedelea, V. Lazureanu, O. Suciu, T. O. Popa and E. Butnaru, *Rev. Chim.*, 2018, **69**, 627.
16 F. F. A. Aziz, A. A. Jalil, S. Triwahyono and M. Mohamed, *Appl. Surf. Sci.*, 2018, **455**, 84.
17 H. Beitollahi and S. Nekooei, *Electroanalysis*, 2016, **28**, 645.
18 M. S. Ahmad, I. M. Isa, N. Hashim, S. M. Si and M. I. Saidin, *J. Solid State Electrochem.*, 2018, **22**, 2691.
19 P. Riederer, *Nutr. Metab.*, 1980, **24**, 417.
20 Á. Sánchez-Ferro, J. Benito-León and J. C. Gómez-Esteban, *Front. Neurol.*, 2013, **4**, 64.
21 L. A. Conlay, T. J. Maher and R. J. Wurtman, *Brain Res.*, 1985, **333**, 81.
22 M. Hinz, A. Stein and T. Uncini, *Int. J. Gen. Med.*, 2011, **4**, 165.
23 M. Miura and N. Takahashi, *Drug Metab. Pharmacokinet.*, 2016, **31**, 12.
24 T. Lapainis, C. Scanlan, S. S. Rubakhin and J. V. Sweedler, *Anal. Bioanal. Chem.*, 2007, **387**, 97.
25 Y. D. Lu, D. C. Lu, R. Y. You, J. L. Liu, L. Q. Huang, J. Q. Su and S. Y. Feng, *Nanomaterials*, 2018, **8**, 400.
26 R. Ramya, P. Muthukumaran and J. Wilson, *Biosens. Bioelectron.*, 2018, **108**, 53.
27 K. Varmira, G. Mohammadi, M. Mahmoudi, R. Khodarahmi, K. Rashidi, M. Hedayati, H. C. Goicoechea and A. R. Jalalvand, *Talanta*, 2018, **183**, 1.
28 E. Molaakbari, A. Mostafavi, H. Beitollahi and R. Alizadeh, *Analyst*, 2014, **139**, 4356.
29 K. Movlaee, H. Beitollahi, M. Reza and P. Norouzi, *Microchim. Acta*, 2017, **184**, 3281.
30 S. Iijima, *Nature*, 1991, **354**, 56.
31 Z. Zhu, *Nano-Micro Lett.*, 2017, **9**, 25.
32 Y. Y. Sun, Q. X. Ren, X. Liu, S. Zhao and Y. Qin, *Biosens. Bioelectron.*, 2013, **39**, 289.
33 H. Y. Sun, Z. Xu and C. Gao, *Adv. Mater.*, 2013, **25**, 2554.
34 J. B. Raoof, R. Ojani, M. Amiri-Aref and M. Baghayeri, *Sens. Actuators, B*, 2012, **166–167**, 508.
35 M. Baghayeri and M. Namadchian, *Electrochim. Acta*, 2013, **108**, 22.
36 T. R. Silva, A. Smaniotto and I. C. Vieira, *J. Solid State Electrochem.*, 2018, **22**, 1277.
37 M. Amiri-Aref, J. B. Raoof and R. Ojani, *Sens. Actuators, B*, 2014, **192**, 634.
38 F. F. Hudari, E. H. Duarte, A. C. Pereira, L. H. D. Antonia, L. T. Kubota and C. R. T. Tarley, *J. Electroanal. Chem.*, 2013, **696**, 52.
39 Y. Fan, J. Liu, H. Lu and Q. Zhang, *Microchim. Acta*, 2011, **173**, 241.
40 M. Taei and G. Ramazani, *Colloids and Surfaces B: Biointerfaces*, 2014, **123**, 23.
41 T. Madrakian, E. Haghshenas and A. Afkhami, *Sens. Actuators, B*, 2014, **193**, 451.

